Neutron and X-ray diffraction study of cubic [111] field cooled Pb(Mg$_{1/3}$Nb$_{2/3}$)O$_3$

C. Stock,[1] Guangyong Xu,[2] P. M. Gehring,[3] H. Luo,[4] X. Zhao,[4] H. Cao,[5] J.F. Li,[5] D. Viehland,[5] and G. Shirane[6]

[1]*Department of Physics and Astronomy, Johns Hopkins University, Maryland, 21218*
[2]*Condensed Matter Physics and Materials Science Department,*
Brookhaven National Laboratory, Upton, New York, 11973
[3]*NIST Center for Neutron Research, National Institute of Standards and Technology, Gaithersburg, Maryland, 20899*
[4]*Shanghai Institute of Ceramics, Chinese Academy of Sciences, Shanghai, China, 201800*
[5]*Department of Materials Science and Engineering, Virginia Tech., Blacksburg, Virginia, 24061*
[6]*Physics Department, Brookhaven National Laboratory, Upton, New York, 11973*
(Dated: February 2, 2008)

Neutron and x-ray diffraction techniques have been used to study the competing long and short-range polar order in the relaxor ferroelectric Pb(Mg$_{1/3}$Nb$_{2/3}$)O$_3$ (PMN) under a [111] applied electric field. Despite reports of a structural transition from a cubic phase to a rhombohedral phase for fields E > 1.7 kV/cm, we find that the bulk unit cell remains cubic (within a sensitivity of 90°-α =0.03°)for fields up to 8 kV/cm. Furthermore, we observe a structural transition confined to the near surface volume or 'skin' of the crystal where the cubic cell is transformed to a rhombohedral unit cell at T$_c$=210 K for E > 4 kV/cm, for which 90°-α=0.08 $\pm$ 0.03° below 50 K. While the bulk unit cell remains cubic, a suppression of the diffuse scattering and concomitant enhancement of the Bragg peak intensity is observed below T$_c$=210 K, indicating a more ordered structure with increasing electric field yet an absence of a long-range ferroelectric ground state in the bulk. The electric field strength has little effect on the diffuse scattering above T$_c$, however below T$_c$ the diffuse scattering is reduced in intensity and adopts an asymmetric lineshape in reciprocal space. The absence of hysteresis in our neutron measurements (on the bulk) and the presence of two distinct temperature scales suggests that the ground state of PMN is not a frozen glassy phase as suggested by some theories but is better understood in terms of random fields introduced through the presence of structural disorder. Based on these results, we also suggest that PMN represents an extreme example of the two-length scale problem, and that the presence of a distinct skin maybe necessary for a relaxor ground state.

PACS numbers: 77.80.-e, 61.10.Nz, 77.84.Dy

I. INTRODUCTION

The relaxor ferroelectrics have attracted considerable interest due to their unique dielectric properties and exceptionally large piezoelectric coefficients.[1,2,3,4] Pb(Zn$_{1/3}$Nb$_{2/3}$)O$_3$ (PZN) and Pb(Mg$_{1/3}$Nb$_{2/3}$)O$_3$ (PMN) are prototypical relaxors which, under zero field cooling, show a broad and frequency dependent peak in the dielectric constant but no well defined structural transition. The broad anomaly of the dielectric response is reflected in the phonon spectra where a soft transverse optic mode softens and then recovers with decreasing temperature.[5] Concurrent with the recovery of the soft-optic mode, strong diffuse scattering is observed along the $\langle 110 \rangle$ directions, indicative of short-range ferroelectric order, which persist to low temperature. Measurements using neutron pair distribution function analysis have confirmed that at low temperatures no long-range polar order is present with a maximum of $\sim$ 1/3 of the sample having polar order.[6]

Under the application of a strong electric field, a sharp and frequency-independent peak in the dielectric response is observed to remain after the removal of the electric field at low temperatures indicative of a well defined structural distortion.[7] However, NMR measurements have shown that it is difficult to associate this with the presence of a long-ranged ferroelectric ground state as two components are measured in the NMR lineshape and at least half of the crystal remains in an disordered state.[8] Dielectric measurements have found the presence of a frozen glassy state at low temperatures and have led to theories of random bond and field effects in analogy to the case of spin glasses.[9,10,11,12]

Recent neutron and x-ray scattering studies conducted on PMN and PZN in zero field have found no long-range structural distortion in the bulk at low temperatures. This new phase (referred to as phase-X in the original measurements) was first measured and presented based on neutron diffraction measurements on PZN doped with 8% PT.[13,14] Instead of long-range ferroelectric order, strong anisotropic diffuse scattering around the Bragg peaks starts near the same temperature where index of refraction measurements indicate that local polar regions are formed.[15,16] Several models describing the diffuse scattering in terms of phase-shifted polar nanoregions and static strain fields have been proposed.[17,18,19,20] We emphasize that all of these models relate the diffuse scattering to the presence of polar correlations in the material. Therefore investigating the effects of an external electric field on the diffuse scattering, direct information of the local polar correlations can be obtained.

The diffuse scattering, the lattice dynamics, and the dielectric response in the relaxors PMN and PZN can be described by two temperature scales. At a high tempera-

ture (T_d), short-range polar correlations begin to develop giving rise to strong diffuse scattering measured through the neutron and x-ray elastic scattering cross sections. The phonons also broaden in energy significantly for temperatures below this onset, which is indicative of very short lifetimes and strong damping.[21] Upon cooling below Tc (defined as the temperature where a sharp dielectric peak is observed under an applied field), the phonons begin to sharpen in energy and their frequencies harden while the diffuse scattering persists. Understanding the response of the diffuse scattering to an electric field as a function of temperature is central to understanding the role of T_c in the structure of PMN. We note that in PMN T_c=210 K and T_d ∼690 K.

Recent electric field studies of pure PZN and PZN-8% PT have shown several interesting results.[22] Upon cooling below T_c, the diffuse scattering intensity is redistributed along different ⟨110⟩ directions while the integrated intensity is conserved. Like the induced polarization, the redistribution of the diffuse scattering persists at low temperatures after removal of the field, which suggests that there is a direct connection between it and the formation of ferroelectric macro-domains under field. Extensive research investigating the shape of the unit cell under the application of an electric field near the morphotropic phase boundary has been presented elsewhere.[23] In the case of pure PMN, previous work has shown a suppression of neutron diffuse scattering intensities occurs in the direction transverse to $\vec{Q}$ across various Bragg peaks with the application of a [110] field, but no correlation between this effect and the presence of ferroelectric domains and/or lattice distortions has been studied.[24]

In this paper we will show that the electric field reduces the diffuse scattering in PMN and enhances Bragg peak intensities at low temperatures, while the unit cell shape remains cubic in the bulk for field strengths up to 8kV/cm. In contrast to previous experiences with PZN and PZN-8%PT, there is no field memory effect as the diffuse scattering and Bragg peak intensities recover their zero-field cooled values at low temperatures immediately upon removal of the external field. Low-energy x-ray diffraction measurements, which probe the skin of the sample, demonstrate that the near-surface region does undergo a structural transition from a cubic to rhombohedral phase. The distortion remains after removal of the field at low-temperatures and therefore displays the expected memory effect based on dielectric and polarization measurements. Our results illustrate that at low temperatures the long-range atomic order, i.e., correlations between polar domains, can be enhanced by an external field. However the intrinsic structural disorder prevents a phase transition from occurring to a long-range ferroelectric state.

This paper is divided into two sections. In the first section we present cold and thermal neutron data that characterize the diffuse scattering (and hence the short-range polar correlations) around the $\vec{Q}$=(001) and $\vec{Q}$=(003) re-
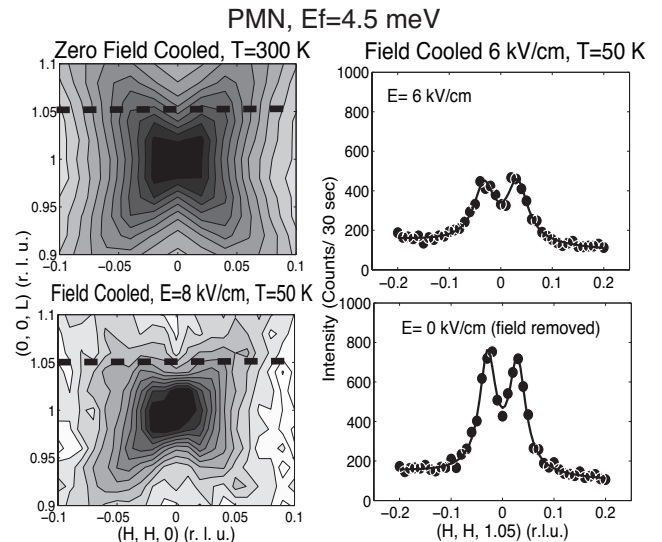

FIG. 1: The diffuse scattering in zero field cooled and field cooled states around the (001) Bragg peak. The dark regions represent high intensity contours in comparison to lighter regions. The dashed lines illustrate the line scans conducted to investigate the temperature dependence of the intensity.

ciprocal lattice positions as a function of electric field. The second section deals with the possibility of a structural distortion. We use neutrons (which probe the entire crystal volume) to study the shape of the bulk unit cell, and low-energy x-rays to study the shape of the unit cell near the surface of the crystal.

II. EXPERIMENT

Neutron scattering experiments were conducted at the BT9 thermal and SPINS cold triple-axis spectrometers located at the NIST Center for Neutron Research on a 1 cm × 1 cm × 0.1 cm plate aligned in the (HHL) scattering plane. Sputtered gold electrodes allowed an electric field to be applied along the [111] direction and independent polarization measurements have revealed a non-zero polarization at low temperatures after field cooling, consistent with previous work.[7,25] The electric field was measured during the experiments through the use of two wires attached in locations different from the two wires driving the voltage difference across the crystal. The measured voltage was always the same as that applied at the power supply. Field cooling sequences were done by first heating the sample to temperatures between 550-600 K then cooling in an applied electric field. This temperature range was chosen to avoid possible decomposition of the sample while still reaching temperatures where the diffuse scattering is nearly entirely suppressed.

During thermal neutron measurements, two different experimental configurations were used to investigate the structure and diffuse scattering both of which employed

a PG(002) monochromator fixed to reflect 14.7 meV (λ=2.36 Å) neutrons. To optimize the momentum transfer resolution $\delta q/Q$ of the structural measurements, the horizontal beam collimations were set to (listed in order from the reactor wall to the detector and where S refers to the sample) 10′-40′-S-20′-*open* and the d-spacing of the (111) PMN Bragg peak was matched with that of the (111) Bragg peak of a perfect SrTiO$_3$ analyzer for which $\delta q/Q \sim 10^{-4}$.[26] During the diffuse scattering measurements, the horizontal beam collimations were set to 40′-40′-S-40′-80′ and a PG(002) crystal was used as an analyzer. This latter configuration provided significantly broader resolution in momentum and was used only to study the diffuse scattering and Bragg peak intensities. A Pyrolytic Graphite filter was placed before the monochromator to remove higher order neutrons. Cold neutron measurements of the diffuse scattering were conducted on the SPINS triple-axis spectrometer with collimations set to *guide*-80′-S-80′-*open*. The neutron final energy was set to 4.5 meV (λ=4.26 Å) and cold Beryllium filters were placed before and after the sample to remove higher order neutrons reflected off the monochromator. The absorption of the neutron beam was negligible in this experiment and therefore the neutron diffraction measurements provided a means of investigating the bulk properties of the PMN crystal.

X-ray experiments were conducted at the X22A beamline at the National Synchrotron Light Source, Brookhaven National Laboratory using an incident photon energy of 10.7 keV. A displex was used to control the sample temperature. The x-ray measurements were done in a reflection geometry and we estimate the penetration depth of the beam to be ~ 15 μm. The x-ray measurements therefore provide a means of studying the properties of the near surface region whereas neutrons probe the entire bulk crystal volume. To characterize the skin volume in more detail we conducted several measurements using a 32 keV x-ray beam (with a penetration depth of 50 μm) which gave results consistent with those obtained using a 10.7 keV beam as discussed below. The x-ray results were reproduced on a smaller crystal (0.5 cm $\times$ 0.5 cm $\times$0.1 cm) from the same boule as the larger crystal used for neutrons. Measurements on this smaller sample gave the same results as that measured on the larger sample, and will not be presented here.

III.   DIFFUSE SCATTERING

Two sets of diffuse scattering measurements were conducted on PMN under an electric field. Measurements on SPINS using cold neutrons focussed on the temperature dependence and lineshape of the diffuse scattering near $\vec{Q}$=(001). Measurements using thermal neutrons on BT9 were conducted near $\vec{Q}$=(003) where the diffuse scattering cross section is nearly an order magnitude larger allowing the low-temperature lineshape to be investigated further in reciprocal space from the Bragg peak. The
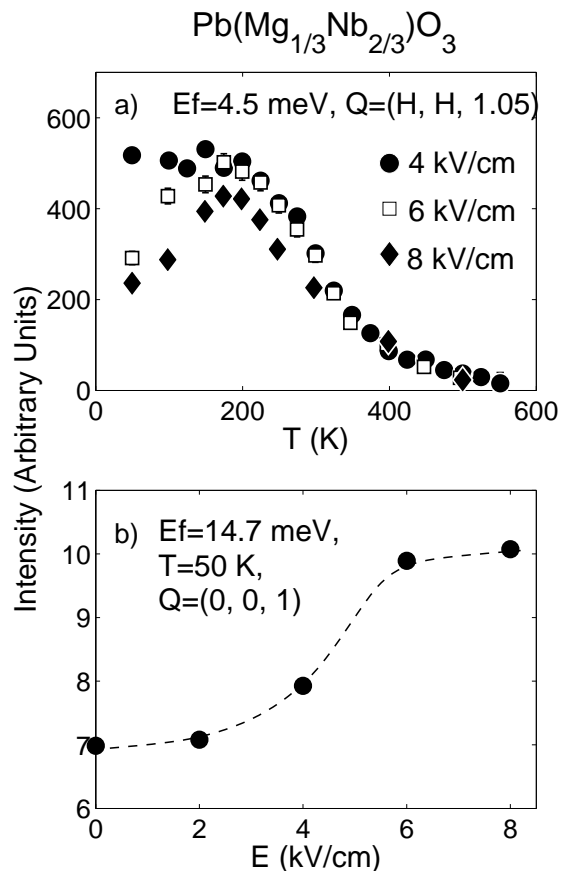

FIG. 2: a) The temperature dependence of the diffuse scattering is plotted for several field cooled values. Panel b) illustrates the Bragg peak intensity as a function of applied electric at 50 K.

possibility of hysteresis and long time constants was investigated on the BT9 thermal triple-axis spectrometer near $\vec{Q}$=(003).

A.   Diffuse Scattering near $\vec{Q}$=(001)

To measure the temperature dependence of the diffuse scattering under the application of an electric field we have studied the diffuse scattering near the $\vec{Q}$=(001) Bragg peak with cold neutrons. Fig. 1 shows contours of constant diffuse scattering intensity measured in the (HHL) scattering plane near the (001) Bragg reflection and representative linear scans through the two diffuse scattering rods. In zero field, the diffuse scattering exhibits a symmetric butterfly-shape as previously observed with both x-rays and neutrons and grows with cooling.[27] Under the application of an electric field oriented along the [111] direction, a change in the diffuse scattering is observed where the diffuse scattering perpendicular to the applied electric field is preferentially suppressed. We

emphasize that the diffuse scattering does not disappear, but it is substantially reduced relative to zero-field cooled values.

Figure 1 also shows scans through the diffuse streaks around $\vec{Q}=(001)$. The two right hand panels show scans taken after field cooling in a 6 kV/cm field. The diffuse scattering is initially suppressed after field cooling (upper panel), however, on removal of the electric field (lower panel), the intensity returns to the value obtained under zero field cooling conditions. Contrary to previous expectations based on conventional ferroelectrics, this effect does not show any electric field history dependence. Upon removal of the electric field at low temperature, the diffuse intensity immediately returns to the zero-field cooled values. This point will be discussed and quantified in more detail in the next section, which deals with the strong diffuse cross section near $\vec{Q}=(003)$. Further measurements show that zero-field cooling the sample to low temperatures and then applying an electric field has the same affect as field cooling (in the same field strength).

In Fig. 2 we plot the temperature dependence of the diffuse scattering under several strong electric fields. The data shown are the intensities of linear scans along the (H,H,1.05) direction. The intensities were extracted by fitting each linear scan to two symmetric Lorentzians displaced equally from the H=0 position. Typical fits are shown in the right hand panels of Fig. 1. The diffuse scattering is onset near the Burns temperature and appears to be insensitive to the application of an electric field at high temperatures. Below the critical temperature $T_c=210$ K, the diffuse scattering is strongly suppressed with increasing electric field, while the (111) Bragg peak intensity increases (with field). The suppression of the diffuse scattering accompanied by the enhancement of the Bragg peak intensity suggests that the total scattering is conserved and that the long-range (Bragg) and short-range (diffuse) polar correlations are strongly coupled. Therefore, as the short-range polar order is suppressed (characterized by a reduction in the diffuse scattering) an increase in long-range correlations is observed (evidenced by the Bragg peak intensity). This situation is different from that proposed in PZN doped with 8% PT where it was suggested that a redistribution of the diffuse scattering occurs.[28]

These results demonstrate the presence of two distinct temperature scales. At high temperatures above T_d there is no diffuse scattering due to the lack of short-range polar correlations, while just below T_d such diffuse scattering is unaffected by an electric field. At lower temperature (below T_c), the application of an electric field reduces the diffuse scattering and increases the Bragg peak intensity. The existence of two characteristic temperature scales is an important observation that is predicted by random field models of the relaxor ferroelectrics. Even though some evidence for the two temperature scales has been observed by investigating the phonons in PMN, a clear structural signature has been lacking. An important question is whether all the diffuse
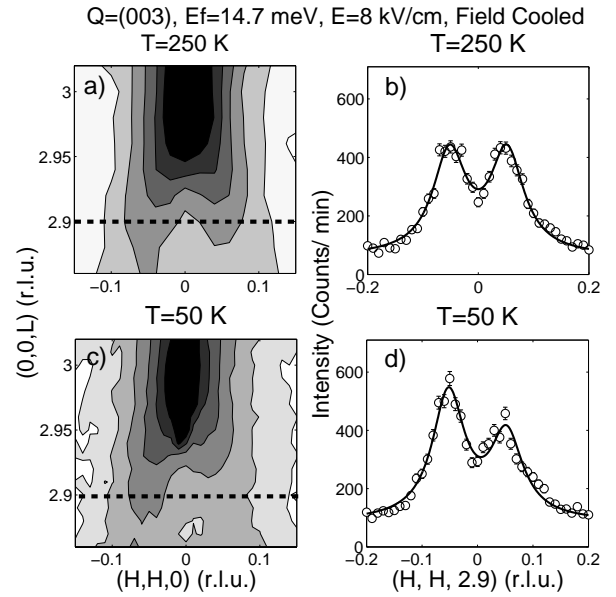

FIG. 3: The diffuse scattering near $\vec{Q}=(003)$ under the application of an 8 kV/cm electric field along [111]. The left hand side shows diffuse contours plotted on a logarithmic scale at temperatures above (250 K) and below (50 K) T_c. The dark regions represent high intensity contours in comparison to lighter regions. The right-hand panels display linear scans through the diffuse scattering and are represented by the dotted line in the contour plots.

scattering is suppressed uniformly in reciprocal space, or one of the streaks or "wings" is preferentially suppressed as the data in the Fig. lower left panel of 1 seem to suggest. To answer these questions in more detail, we study the diffuse scattering around $\vec{Q}=(003)$.

B. Diffuse Scattering near $\vec{Q}=(003)$

To analyze the electric field effect on the diffuse lineshape, i.e. the dependence on the momentum transfer q (defined as the reduced momentum transfer measured relative to the Bragg peak) we have studied the scattering near $\vec{Q}=(003)$ using thermal neutrons on the BT9 triple-axis spectrometer. The q dependence is plotted in Fig. 3 under field cooled conditions (E=8 kV/cm) and at 250 K and 50 K (panels a) and c) respectively). Data at large momentum transfers (i.e. $L \sim 3$) were not obtained due to mechanical limits on the maximum scattering angle of the spectrometer. Examples of linear scans are represented on the right hand panels b) and d). These scans were conducted both above and below the critical temperature $T_c=210$ K.

The data above T_c at 250 K form the symmetric "butterfly" shape centered around $\vec{Q}=(001)$ and are discussed above. Below T_c at 50 K, one wing of the butterfly is diminished as seen near (001) in the lower left panel of
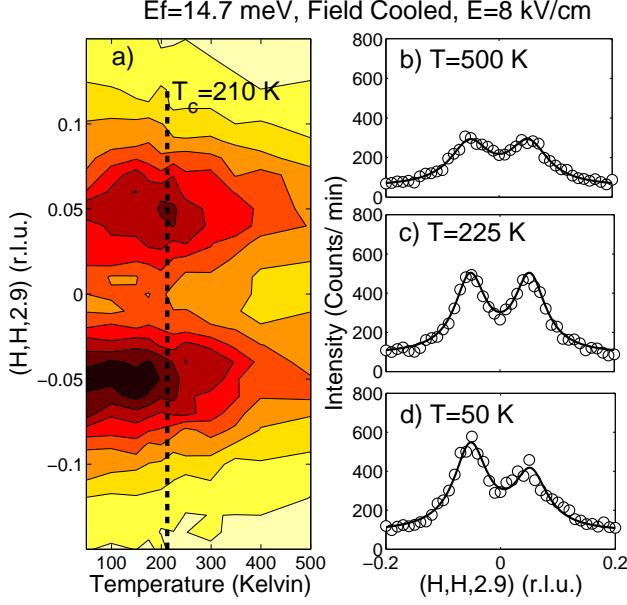
Ef=14.7 meV, Field Cooled, E=8 kV/cm

FIG. 4: (Color online) The temperature dependence of the diffuse scattering near $\vec{Q}=(003)$. Panel a) is a contour plot (on a linear scale) of scans along (H,H,2.9) measured in a field of 8 kV/cm as a function of temperature. The dark regions represent contours of high intensity compared with lighter regions. Panels b) through d) show examples of linear scans at 500 K, 225 K, and 50 K. The panels show the suppression of one wing of the diffuse scattering at T_c.

Fig. 1; however the larger diffuse scattering structure factor near $\vec{Q}=(003)$ provides a boost in intensity that allows the asymmetric lineshape to be observed much more clearly because we can then measure the diffuse scattering further away from the Bragg peak position. The asymmetric "butterfly" shape is clearly confirmed by the two linear q-scans measured along the (H,H,2.9) direction illustrated in panels b) and d). At 250 K, two symmetric peaks are observed, however at 50 K, one peak is suppressed.

The temperature dependence of the field-cooled diffuse scattering near $\vec{Q}=(003)$ is illustrated in Fig. 4 as measured by linear scans along the (H,H,2.9) direction. Example linear scans are represented in panels b), c), and d). The scans show symmetric peaks displaced from the $H=0$ position above $T_c=210$ K and an asymmetric lineshape at low temperatures (below T_c) representing the fact that one of the wings of the diffuse scattering is diminished more than the other. A contour plot of the temperature dependence is illustrated in panel a). The contour plot shows the growth of the diffuse scattering wings above T_c as measured near $\vec{Q}=(001)$, however the plot shows that the asymmetry in the diffuse lineshape is onset at T_c. Therefore, at T_c under field cooled conditions, the diffuse scattering is reduced preferentially along directions perpendicular to the applied electric field.

This feature was not obvious near $\vec{Q}=(001)$ due to the

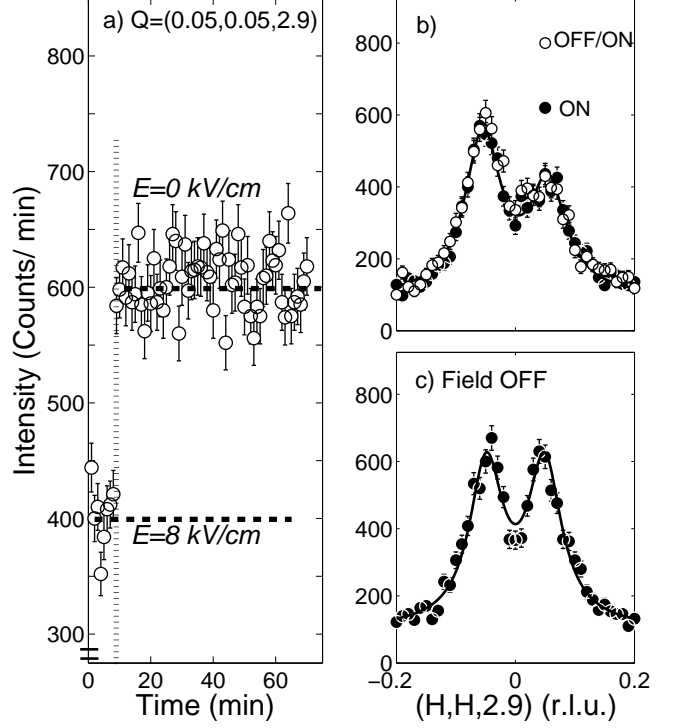Ef=14.7 meV, Field Cooled, T=50 K, E=8 kV/cm

FIG. 5: Panel a) plots the diffuse scattering intensity at $\vec{Q}=(0.05,0.05,2.9)$ as a function of time. The electric field was abruptly turned off and the leads electrically shorted to ground at the time indicated by the dashed line. Panels b) and c) show examples of linear scans of the diffuse scattering before and after the field is turned off. The open circles in Panel b) show the diffuse scattering measured with the field turned back on ∼ 70 minutes after the field was turned off. The diffuse scattering reproduces the field cooled intensity.

fact that the measurements there were conducted closer to the Bragg peak and therefore less sensitive to changes in the lineshape. The increased intensity of the diffuse scattering near (003) has allowed us to investigate the diffuse scattering further away from the Bragg peaks and therefore characterize the lineshape in more detail. The lineshape change can be understood in terms of domains and by noting that the diffuse intensity is proportional to $(\vec{Q}\cdot\vec{\epsilon})^2$, where $\vec{Q}$ is the momentum transfer and $\vec{\epsilon}$ is the polarization vector. Domains with polarization antiparallel to the applied field are not able to rotate and align with the field due to the huge energy required for a 180° rotation. However, domains for which the polarization is at a significantly smaller angle (less than 90°), require a much smaller energy to align with the applied field. This distinction is reflected in the data at high electric fields.

We have also investigated the possibility of the existence of a long time scales and slow dynamics to the diffuse scattering near $\vec{Q}=(003)$ where the diffuse scat-

tering is strong. Long time-scales have been observed in some examples of model magnetic systems in random fields and in particular the case of $Fe_{0.5}Zn_{0.5}F_2$ which is representative of a random field Ising model.[29,30,31] Long time scales were found to exist when the applied magnetic field (which in turn causes the presence of a random field as outlined by Fishman and Aharony in Ref. 32) was turned on at low temperatures below the ordering transition. It is not clear in our case if the same situation would apply as the random fields are presumably introduced through structural disorder and hence present at all temperatures and at all applied electric fields. Long time dependences have been measured in the birefringence and structural properties (characterized with low-energy x-rays) in PMN (Ref. 10,33,34), in the relaxor SBN (Ref. 36), and $KTaO_3$ doped with 3% Li (37). Our data for PMN is illustrated in Fig. 5. Panel a) plots the time dependence of the intensity at $\vec{Q}=(0.05,0.05,2.9)$ which (as can be seen from Fig. 3), corresponds to the peak of one of the diffuse scattering wings. The temperature in Fig. 5 is 50 K and the sample was cooled in an 8 kV/cm from high temperature. At time $t = 0$ the sample is in a field cooled state and then the field was turned off and the surfaces of the crystal electrically grounded at the time indicated by the dotted line. The diffuse scattering intensity rose abruptly and did not change for another hour of measurements. Linear scans showing the diffuse scattering intensity when the electric field was on (field cooled and at a time before that indicated by the dotted line in Fig. 5) and then off (after waiting for about 1 hour after the field was turned off and crystal faces electrically shorted to ground) are represented in panels b) and c) respectively by the filled circles. After turning the electric field off for over an hour, we then turned it back on at 50 K and the resulting profile is represented by the open circles in panel b). The diffuse intensity tracks the original intensity obtained under field cooling conditions within error. We note that the Bragg peak intensity responded similarly but with an increase in intensity on application of the electric field, and subsequent decrease on removal (as expected given our measurements made near $\vec{Q}=(001)$). We therefore conclude from this sequence, that there are no long time scales associated with the electric field effects measured here.

The lack of any time dependence contrasts with that found using birefringence and x-rays in PMN (Ref. 10,33,34) and also neutron diffraction measurements on PZN doped with PT (Ref. 22). Doping with PT has been snown to stabilize the rhombohedral phase in PMN and related materials; therefore the rhombohedral phase and the resulting effects on the diffuse scattering maybe more easily frozen in for those systems. The birefringence measurements are more difficult to reconcile, however, we emphasize that with neutrons we are measuring at a non zero wave vector associated with a certain length scale. The length scales studied with neutrons and the expected size of the polar nanoregions have been discussed by Vugmeister.[38] In the case of the linear scans

measured along (H,H,2.9) we would expect to study polar correlations with a length scale $\lambda \sim 1/q \sim 6$ Å, which is a very short length scale compared to other techniques. It therefore is possible that the time dependence measured with birefringence is associated with longer length scales than investigated here. Indeed, studies on the history dependence of PMN doped with PT have found domain formation and history dependence associated with length scales as large as millimeters.[39,40] Our neutron diffraction experiments are not sensitive to such long length scales. These conflicting results may also indicate the presence of two different behaviors for the bulk and surface. Neutrons probe the bulk where optical techniques are confined to a surface skin region. This point is investigated in the next section (and is compared directly with x-ray measurements similar to those conducted in Refs. 33,34), which discusses the shape of the unit cell and structural properties.

The absence of any history dependence suggests that the ground state of PMN under field cooling is not a glassy state nor in a well defined ferroelectric ground state.[35] Here long-range and short-range polar order coexists and compete with each other. Similar measurements on single crystals of PZN and PZN-8%PT do not show a suppression of diffuse scattering intensities, but only a redistribution with field history dependence. One distinct difference between PMN and PZN is that in the latter, long range rhombohedral domains form with an external [111] field. Therefore the memory effect of diffuse scattering measured in PZN and PZN-8%PT is more likely to be associated with ferroelectric domain formation and rotation.

The electric field effects show that there is a direct relation between the polar correlations and the diffuse scattering. The fact that the diffuse scattering is only diminished below T_c and, in particular, very anisotropic (being elongated strongly along one direction) and exhibits no memory is suggestive that the diffuse scattering is directly related to the polar structure in the relaxor ferroelectrics as described in several models.[19,41]

An important result is that our measurements show a *clear structural signature* of two distinct temperature scales. At a high temperature, the diffuse scattering is onset and is insensitive to the application of an electric field. Presumably, in this temperature range the polar moments are isotropic and insensitive to the presence of a strong electric field which selects a particular direction. This suggests that the polar moments have a continuous symmetry between the temperature range T_d and T_c. In analogy to spins in magnetic systems, the Hamiltonian in this temperature range can be approximated by Heisenberg component. Below T_c, the situation and the underlying Hamiltonian change as evidenced by both a decrease in the diffuse scattering intensity and the asymmetric lineshape measured near $\vec{Q}=(001)$ and (003). Both the decreases in intensity and asymmetry are onset at T_c. This suggests a change in the universality class as the polar moments have a strong anisotropy im-

plying that a discrete symmetry is dominating the ground state Hamiltonian, as is the case for a cubic anisotropy term in the Hamiltonian. Given that the same Hamiltonian must apply at all temperatures, these results show that T_c characterizes the cubic anisotropy in the Hamiltonian, while T_d describes the continuous (Heisenberg) component of the Hamiltonian. Therefore, PMN is a system where the energy scale of the continuous component of the Hamiltonian dominates over the anisotropic component. The dominant term (and hence the effective universality class) can be tuned with temperature.

PMN (and indeed all relaxors) exhibit a significant amount of structural disorder as a result of the mixture of two different ions with different valency. In the case of PMN, we expect there to be a random field introduced as a result of the mixture between Mg^{2+} and Nb^{5+} ions.[42] Random fields have very different effects on universality classes with discrete and continuous symmetries as summarized in the work by Imry and Ma.[43] For the case of discrete symmetry (for example in PMN below T_c where a strong cubic anisotropy dominates), the system should be less sensitive to the formation of random fields and long-range polar correlations are predicted to develop. In the case of a continuous symmetry (as in PMN above T_c) the correlations should be strongly affected and short ranged in the presence of a random field. These two cases are reflected in our data with long-range polar correlations only developing below T_c as evidenced by an enhancement of the Bragg peak intensity.

Random field models of relaxors predict two distinct temperature scales associated with a high-temperature transition and then a low-temperature cross over point where the universality class changes from being Heisenberg to Ising like in analogy with model magnetic systems.[44,45] While it was suggested that the phonon spectrum may well reflect the two temperature scales required by such a model, the structural properties remain ambiguous as the diffuse scattering from the bulk (measured with neutrons) in PMN shows little sign of T_c and PZN is heavily contaminated by a large surface effect. We note that low-energy x-ray measurements probing the surface of PMN have found evidence for an anomaly of the diffuse scattering intensity near T_c.[46] No such clear anomaly is observed in our neutron data. The two temperature scales required by random field models are reflected in the diffuse scattering intensity as a function of temperature under the application of a strong electric field. At high temperatures where the universality class is Heisenberg, random fields destroy the phase transition and short-range correlations are formed. It is only at T_c, where the system crosses over to an Ising universality class, that the phase transition becomes robust to random fields and long-range correlations can develop. We note that this model still requires further verification as some measurements have found evidence for more than two temperature scales in PMN.[46] It maybe that some of these temperature scale can be reconciled based on the dynamics and the energy resolution of the experimental
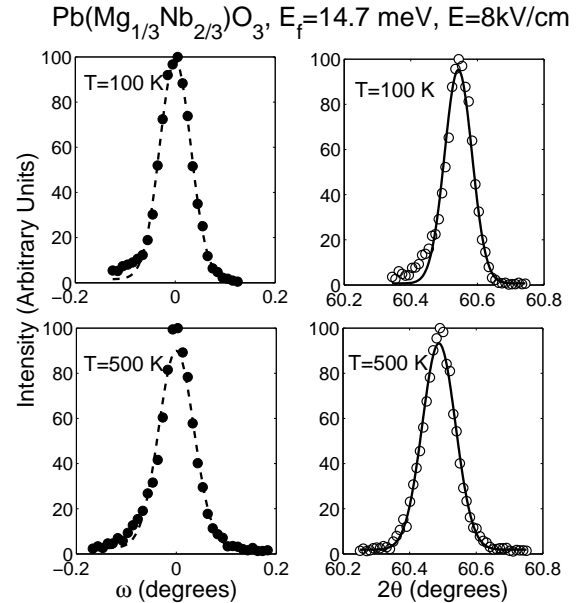

FIG. 6: Longitudinal $(\theta - 2\theta)$ and transverse (ω) scans through the (111) Bragg peak at 100 K and 500 K are displayed. No strong distortion at low temperatures is observed.

probe, however further experimental work is required to investigate this point.

IV. STRUCTURAL PROPERTIES

Two sets of experiments were conducted under field cooling conditions to search for a structural distortion under an electric field in field cooling conditions. To study the bulk properties of the PMN crystal, we have used a high-resolution neutron diffraction setup. For PMN, neutrons have a large penetration depth on the order of $\sim$ 1 cm, therefore providing a bulk probe of the structure. These measurements found no evidence for a structural distortion with a sensitivity estimated at 90°-α= 0.03°.

The second set of measurements were conducted using 10.7 keV x-rays in reflection geometry with a penetration depth of $\sim$ 15 μm.[47] These measurements were aimed at studying the surface properties of the crystal. Evidence for a structural distortion was obtained with 90°-α measured to be $0.08 \pm 0.03°$. We emphasize that these experiments were conducted under field-cooled conditions where the sample was heated to temperatures between 550-600 K (above the onset temperature of the diffuse scattering and the polar correlations) and then cooled under the application of an electric field. This field cooling sequence is very different from that used in previous studies (for example Ref. 33) where the field is applied at room temperature or below the onset temperature of diffuse scattering.

A. Unit cell in the bulk (Neutron diffraction E_f=14.7 meV and SrTiO$_3$ analyzer)

The field effect on the diffuse scattering is strongly correlated with T$_c \sim 210$ K and not the Burns temperature, showing directly that T$_c$ is an important temperature scale below which long-ranged polar correlations are enhanced by the external field. On the other hand, the true origin of the long-range order is controversial. Fig. 6 shows longitudinal scans through the (111) Bragg peak in PMN, measured after field cooling from 600 K. For all electric field strengths up to $E = 8$ kV/cm, we observe no change in the radial lineshape near (111), as opposed to the expected splitting due to a rhombohedral distortion. We have checked other equivalent {111} reflections and have always found a single peak with the same 2θ value (within an error $\pm$ 0.01° based on Gaussian fits) and hence the same d-spacing, ruling out the possibility of a rhombohedral single domain state. We note that all of these measurements were conducted under the field cooling conditions outlined above and low temperature measurements were made after waiting more than 2 hours at low temperatures. This rules out the possibility of a long time dependence and slow response as suggested in some x-ray diffraction studies.[33] This provides definitive evidence that the unit cell shape in pure PMN with field cooling (up to 8kV/cm) to low temperature is still cubic on average, or, much (more than an order of magnitude) less rhombohedral than previously reported[1].

Further confirming the lack of any clear rhombohedral distortion we plot the strain (upper panel) and the longitudinal width measured at the (111) Bragg peak (lower panel) as a function of temperature in Fig. 7. From the temperature dependence, it can be seen that there is no change of the thermal expansion coefficient on the application of an electric field (as discussed in terms of the expected sensitivity of the experiment below). Also, for large fields (8 kV/cm) the strain with temperature is no different to that measured at lower fields. The upper panel shows the lattice strain as a function of temperature taking d_0 to be the unit cell length measured at the given temperature in zero field cooling conditions. The lower panel illustrates the linewidth as a function of temperature. The values are normalized to Γ_0 which is taken as the average value over the entire temperature range studied. Both the lattice strain and the longitudinal width show no strong response to an electric field nor T$_c$. Therefore, we do not observe a clear structural transition to a long-ranged ordered rhombohedral phase at T$_c$.

It is important to establish an upper limit on the sensitivity of the neutron measurements to a rhombohedral distortion and define this quantitatively. One way of characterizing the sensitivity is based on the half-width at half maximum in Fig. 6. If the crystal did undergo a structural distortion, we might expect the Bragg peak to split in the longitudinal direction as measured in a θ-2θ scan at $\vec{Q}$=(111). This splitting would be result of

domains forming with different d-spacings for the (111) and ($\bar{1}$11) Bragg peaks. Since we only observe one peak in any such scan at low temperatures, the half-width at half maximum provides a good measure of the sensitivity to such a scenario. Based on this we put an upper limit of 0.02° for the value of the crystallographic parameter $90° - \alpha$.

Another method of defining the sensitivity of the experiment is to characterize how sensitive the results are to the formation of a single domain state. Such a ground state is not unexpected given the large field strengths applied here. In this case, we would expect an anomaly in the thermal expansion at low temperatures with different domains having different d-spacings (as discussed above). In the upper panel of Fig. 7, the strain is plotted as a function of temperature for field cooling under electric fields of 4 kV/cm and 8 kV/cm. Based on the standard deviation of the data (from the case of no strain which is $d/d_0 - 1$=0) we estimate that the we are sensitive to values of $90°$-$\alpha > 0.03°$.

We have therefore defined the sensitivity of the experiment to the formation of a ground state with domains, and a single domain rhombohedral domain. Based on these two methods for defining the sensitivity of the experiment to a rhombohedral distortion, we therefore expect that the high resolution neutron diffraction measurements are sensitive to distortions greater than $90°$-$\alpha \sim 0.02$-$0.03°$. We note that PMN doped with 27% PT undergoes a transition to a rhombohedral phase with $\alpha \sim 0.18°$ and in the surface of pure PZN, a distortion of $90°$-α=0.085° is measured.[48] PMN doped with 10%PT has been measured to undergo a distortion with $90°$-α=0.13°.[46] In pure PMN, x-ray measurements have found $90°$-α=0.1°.[1] In all cases, we expect that the current experiment would have been able to detect such distortions based on our estimates for the sensitivity.

B. Unit cell in the skin (X-ray diffraction with Ei=10.7 keV and in reflection geometry)

To reconcile our results with previous measurements[1,34], where a rhombohedral distortion was observed in PMN with field cooling, we consider work done on PMN and PZN. It was shown that in both systems there is a "skin" region on the order of tens of microns thick, having a unit cell shape different from that of the bulk.[49,50,51] In zero field, PZN undergoes a structural distortion in the near surface region only.[52] The surface thickness was estimated in these experiments based on the penetration depth of the x-rays used and also using a small narrow neutron beam in a strain scanning geometry.

In Fig. 8, we investigate the possibility that only the near surface region of PMN undergoes a structural distortion in an electric field. To do this we use low-energy x rays in reflection geometry to study the surface of PMN under an electric field. Fig. 8 shows the strain (upper
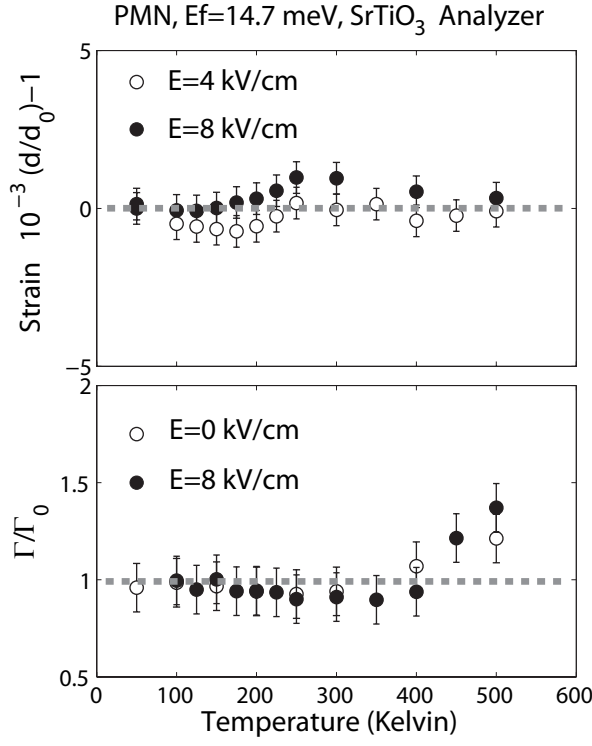
FIG. 7: The lattice strain is plotted in the upper panel as a function of temperature for field cooling with electric fields of 4 and 8 kV/cm. The values for d_0 are taken as the measured lattice constant in zero field cooled conditions at the given temperature. The longitudinal width as a function of temperature for $\vec{Q}=(111)$ Bragg peak is plotted in the lower panel b). No change in the longitudinal linewidth or anomalous strain is observed in the bulk under field cooled conditions.
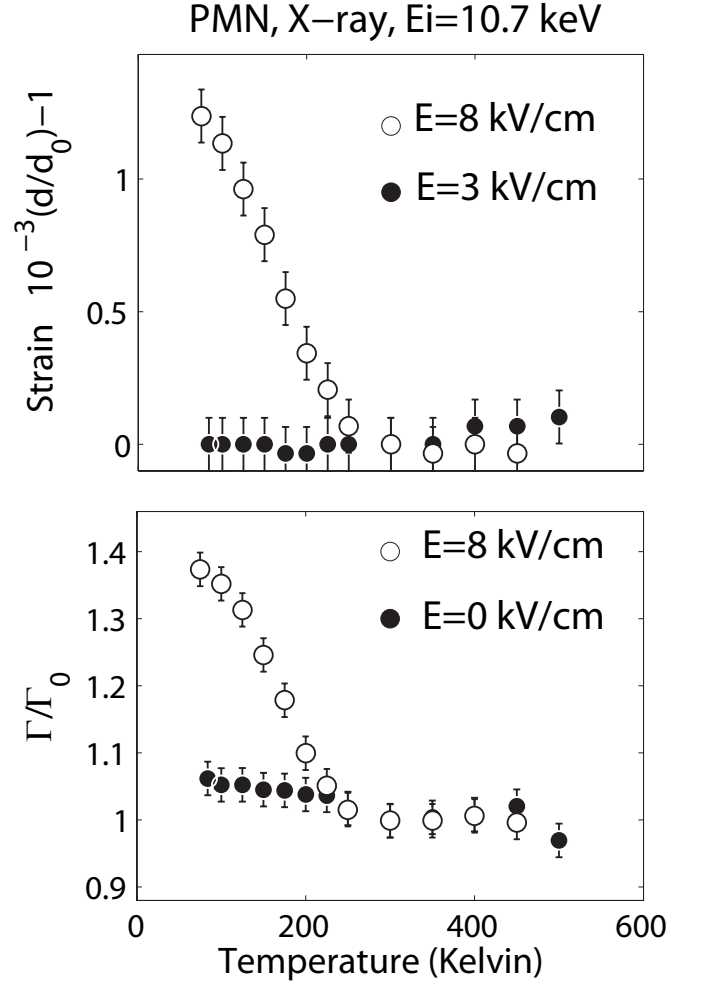
FIG. 8: The lattice strain is plotted in the upper panel as a function of temperature for field cooling with electric fields of 3 and 8 kV/cm. The values for d_0 are taken as the lattice constants measured under zero field cooling conditions at the given temperature. The lower panel plots the linewidth as a function of temperature for cooling under electric fields of 0 and 8 kV/cm. The data shows a clear anomaly in both the lattice strain and the linewidth at T_c for cooling under a 8 kV/cm field.

panel) and longitudinal linewidth (lower panel) of the (111) Bragg peak as a function of temperature for various electric fields. The value of d_0 was taken to be the lattice constant measured at the given temperature under zero field cooling conditions. The linewidth was extracted by fitting the profiles to a Lorentzian raised to the power of 3/2. This lineshape is expected for the case of random fields introduced by domains with the spectrometer integrating the scattering perpendicular to the scattering plane. Here low-energy 10.7 keV x-rays do show a broadening of the Bragg peaks at low-temperatures under field cooled conditions. The results also show the lattice strain grows below T_c under large electric fields, in contrast to neutrons which show no anomaly in the strain around T_c. This is indicative of a structural transition into a more rhombohedrally distorted phase at T_c. Because of the presence of one symmetric peak displaced in 2θ, we interpret this in terms of a single domain state.

Data illustrating the structural distortion in more detail are illustrated in Fig. 9. Panel a) illustrates the lattice strain under field cooling in an 8 kV/cm field, and warming after removal of the electric field at low temperatures. Based on this measurement it can be seen that on

removal of the field at low temperatures, the lattice strain remains but on warming a hysteresis is observed in the response. This effect is expected and has been measured previously in PMN where a rhombohedral distortion was observed at low temperatures.[1,34] Such a memory effect was not observed in the bulk with neutrons and further distinguishes the surface skin layer from the bulk. We also note that on removal of the electric field at low temperatures and heating, the Bragg peaks remained broad and only recovered on warming through T_c. Therefore, the surface region displays the expected memory effect which is absent in the bulk and is similar to previous results using x-rays.

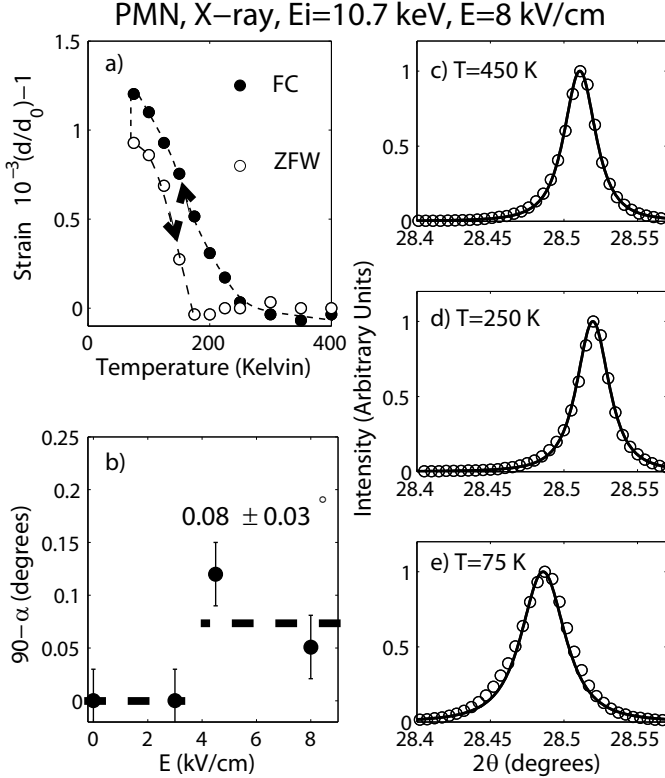Panel b) of Fig. 9 shows the value for α as a function

FIG. 9: Panel a) plots the lattice strain under field cooling (8 kV/cm) and zero field warming conditions. The data shows that the distortion remains on removal of the electric field at low temperatures. Panel b) plots the measured value of α as a function of electric field. Panels c) through e) shows $\theta - 2\theta$ scans through the (111) Bragg peak at 450 K, 250 K, and 75 K.

of applied electric field and shows that at large values of the electric field α=0.08±0.03°. Such a large distortion is well within the sensitivity of our neutron diffraction measurements further emphasizing that the surface undergoes a much stronger distortion than the bulk phase. The values of α are similar to those measured previously in thin crystals of PMN and the temperature at which the distortion is observed, is also consistent with previous data. We note that no such transition was observed in the bulk single crystals with neutrons.

Panels c) through e) of Fig. 9 illustrate raw θ-2θ scans through the (111) Bragg peak using 10.7 keV x-rays. Panels c) and d) are taken at temperatures above T_c=210 K and show the expected decrease of the lattice constant on cooling. However, panel e) shows a scan at low temperatures below T_c and shows that the lattice as expanded. The strain measurements presented in Fig. 8 show that this occurs at T_c and is suggestive of the formation of a single domain rhombohedral ground state.

The x-ray results taken in comparison with the neutron data show that the ferroelectric distortion is confined to the near surface region of the sample. In an effort to determine how thick this skin layer is, we have repeated

the experiment with 32 keV x-rays on the same beamline X22A (NSLS). The penetration depth in this case is ~ 50 μm. These results also showed a structural distortion below T_c with 90°-α=0.06±0.03°. This distortion is within error equal to that obtained with the lower energy x-rays of 10.7 keV. Therefore, the skin layer in PMN is at least 50 μm deep, however our neutron results show it is not characteristic of the bulk.

These results supports the claim that the distortion is limited to a small region near the surface and is not representative of the bulk properties and indicate that the near surface region is sensitive to the application of an electric field. This is in accord with previous x-ray measurements (with a similar penetration depth to the experiments presented here) on PMN which were conducted on 30 μm thick samples and comparable to the estimated thickness of the "skin" layer in our sample.[7,49] Models based on different dual structures for the PZN-xpT phase diagram have been proposed and discussed.[53] Our results are strongly suggestive that anomalies in dielectric measurements may also be dominated by a skin region and not an indicative of the bulk phase. These results are also consistent with recent piezoresponse force microscopy which suggest unusual properties near the surface of PMN-10% PT.[54]

Even though the presence of a surface skin having different critical properties is unusual in materials and condensed matter physics, the effect has been observed before in the case of model magnets in the presence of random fields. The experiments described here are reminiscent of the situation in the three dimensional random field Ising model applied to $Mn_{0.75}Zn_{0.25}F_2$. A series of experiments by Hill $et\ al.$ (Ref. 30) showed the presence of long-range magnetic order in a skin (measured through magnetic x-ray diffraction) in contrast to the bulk which only showed short-ranged magnetic order, exactly the same situation here. Also, there have been many systems which exhibit the two-length scale effect and have a skin which displays different critical behavior than the bulk. Examples include Tb (Ref.55,56), $SrTiO_3$ (Ref. 57), and $CuGeO_3$ (Ref. 58). Possible explanations of the two-length scales have been proposed and a review and discussion can be found elsewhere.[59]

It is interesting to speculate whether the presence of a skin is important (and even necessary) for the presence of a relaxor ground state. Given the many results showing the presence of a distinct skin in relaxors, it maybe that the ferroelectric transition in these systems is driven by the surface boundary condition. Whether this is the result of strain or chemical inhomogeneity at the surface is not clear and further investigation would be required to distinguish these two cases.

It is interesting to note that even when the polar nanoregions are reduced by the field, a long-range (rhombohedral) ferroelectric phase has not been established in the bulk. However, as noted in the section discussing the diffuse scattering, the Bragg peak intensity is enhanced at low temperatures as a function of field implying a more

ordered structure. This occurs while the diffuse scattering is reduced under an electric field. We note that the absence of a long range ferroelectric ground state is supported by recent NMR results which show at least half of the sample remains in a disordered ground state under the application of an electric field as discussed in the introduction.

V. CONCLUSIONS

We have presented a neutron and x-ray scattering study of the diffuse scattering in PMN under the application of a strong electric field. Our results show that the diffuse scattering is directly associated with short-range polar order in the system. The balance between this short-range polar order and long- range atomic order in the bulk of the sample is reflected in a trade off of intensity between the diffuse and Bragg scattering and is tuned with an electric field. However, for fields below 8 kV/cm, no long-ranged ferroelectric phase is formed.

The absence of any hysteresis in the bulk suggests that the ground state of PMN is not a glassy state. Instead, the presence of two temperature scales agrees with predictions of recent random field models proposed for relaxor systems. The results also show that the outer-most tens of microns "skin" layer behaves distinctly different than the bulk (under field).

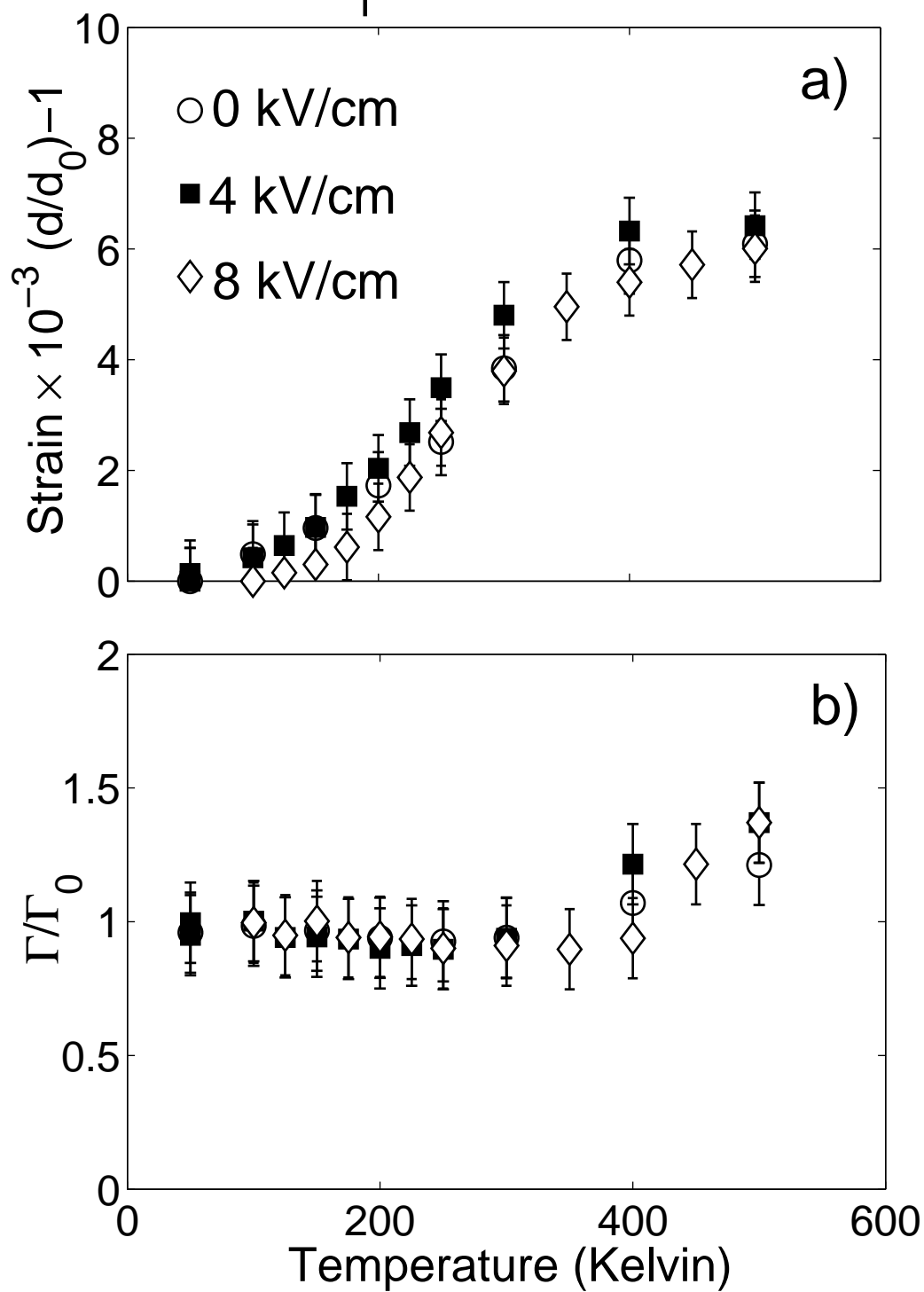[1] Z.-G. Ye, *Key Engineering Materials Vols. 155-156*, 81 (1998).

[2] A.A. Bokov and Z.-G. Ye, J. Mat. Sci. **41**, 31 (2006).

[3] K. Hirota, S. Wakimoto, and D.E. Cox, J. Phys. Soc. Jpn. **75**, 111006 (2006).

[4] S.-E. Park and T.R Shrout, J. Appl. Phys. **82**, 1804 (1997).

[5] S. Wakimoto, C. Stock, R.J. Birgeneau, Z.-G. Ye, W. Chen, W.J.L. Buyers, P.M. Gehring, and G. Shirane, Phys. Rev. B **65**, 172105 (2002).

[6] I.-K. Jeong, T.W. Darling, J.K. Lee, Th. Proffen, R.H. Heffner, J.S. Park, K.S. Hong, W. Dmowski, and T. Egami, Phys. Rev. Lett. **94**, 147602 (2005).

[7] Z.-G. Ye and H. Schmid, Ferroelectrics **145**, 83 (1993).

[8] R. Blinc, V. Laguta, and B. Zalar, Phys. Rev. Lett. **91**, 247601 (2003).

[9] S.N. Gvasaliya, B. Roessli, R.A. Cowley, P. Huber, and S.G. Lushnikov, J. Phys.: Condens. Matter **17**, 4343 (2005).

[10] V. Westphal, W. Kleemann, and M.D. Glinchuk, Phys. Rev. Lett. **68**, 847 (1992).

[11] R. Pirc, R. Blinc, and V.S. Vikhnin, Phys. Rev. B **69**, 212105 (2004).

[12] R. Fisch, Phys. Rev. B **67**, 094110 (2003).

[13] K. Ohwada, K. Hirota, P.W. Rehrig, Y. Fujii, and G. Shirane, Phys. Rev. B **67**, 094111 (2003).

[14] P.M. Gehring, K. Ohwada, and G. Shirane, Phys. Rev. B **70**, 014110 (2004).

[15] G. Burns and F.H. Dacol, Solid State Commun. **48**, 853 (1983).

[16] L.E. Cross, Ferroelectrics **76**, 241 (1987).

[17] S.B. Vakhrushev, A. Ivanov, and J. Kulda, Phys. Chem. Chem. Phys. **7**, 2340 (2005).

[18] K. Hirota, Z.-G. Ye, S. Wakimoto, P.M. Gehring, and G. Shirane, Phys. Rev. B **65**, 104105 (2002).

[19] T.R. Welberry, M.J. Gutmann, H. Woo, D.J. Goossens, G. Xu, C. Stock, W. Chen, Z.-G. Ye, J. Appl. Cryst. **38**, 639 (2005). T. R. Welberry, D. J. Goossens, and M. J. Gutmann Phys. Rev. B **74**, 224108 (2006).

[20] H. You and Q.M. Zhang, Phys. Rev. Lett. **79**, 3950 (1997).

[21] P.M. Gehring, S.-E. Park, and G. Shirane, Phys. Rev. B **63**, 224109 (2001).

[22] G. Xu, P.M. Gehring, and G. Shirane, Phys. Rev. B **72**, 214106 (2005). G. Xu, Z. Zhong, Y. Bing, Z.-G. Ye, and G. Shirane Nature Materials **5**, 134 (2006).

[23] H. Cao, J. Li, and D. Viehland, J. Appl. Phys. **100**, 034110 (2006). H. Cao, J. Li, D. Viehland, and G. Xu Phys. Rev. B **73**, 184110 (2006).

[24] S.B. Vakhrushev, A.A. Naberezhnov, N.M. Okuneva, and B.N Savenko, Phys. Solid State **40**, 1728 (1998).

[25] H.Cao, unpublished (2006).

[26] G. Xu, P.M. Gehring, V.J. Ghosh, and G. Shirane, Acta. Cryst. **A60**, 598 (2004).

[27] H. Hiraka, S.-H. Lee, P.M. Gehring, G. Xu, and G. Shirane, Phys. Rev. B **70**, 184105 (2004).

[28] G. Xu, P.M. Gehring, and G. Shirane, Phys. Rev. B **74**, 104110 (2006).

[29] Q. Feng, R.J. Birgeneau, and J.P. Hill, Phys. Rev. B **51**, 15188 (1995).

[30] J.P. Hill, T.R. Thurston, R.W. Erwin, M.J. Ramstad, and R.J. Birgeneau, Phys. Rev. Lett **66**, 3281 (1991).

[31] J.P. Hill, Q. Feng, Q.J. Harris, R.J. Birgeneau, A.P. Ramirez, and A. Cassanho, Phys. Rev. B **55**, 356 (1997).

[32] S. Fishman and A. Aharony, J. Phys. C **12**, L279 (1979).

[33] S.B. Vakhrushev, J.-M. Kiat, and B. Dkhil, Solid State Comm. **103**, 477 (1997).

[34] G. Calvarin, E. Husson, and Z.G. Ye, Ferroelectrics, **165**, 349 (1995).

[35] X. Zhao, W. Qu, X. Tan, A.A. Bokov, and Z.-G. Ye Phys. Rev. B, **75**, 104106 (2007).

[36] L.K. Chao, E.V. Colla, M.B. Weissman, and D. Viehland, Phys. Rev. B **72**, 134105 (2005).

[37] H. Yokota, Y. Uesu, J. Phys: Condens. Matter **19**, 102201

[37] (2007).

[38] B.E. Vugmeister Phys. Rev. B **73**, 174117 (2006).

[39] F. Bai, J. F. Li, and D. Viehland, J. Appl. Phys. **97**, 054103 (2005).

[40] D. Viehland, J. F. Li, E.V. Colla, J. Appl. Phys. **96**, 3379 (2004).

[41] G. Xu, G. Shirane, J.R.D. Copley, and P.M. Gehring, Phys. Rev. B **69**, 064112 (2004).

[42] W. Kleeman, J. Mat. Sci, **41**, 129 (2006).

[43] Y. Imry and S.K. Ma, Phys. Rev. Lett. **35**, 1399 (1975).

[44] C. Stock, H. Luo, D. Viehland, J. F. Li, I. P. Swainson, R. J. Birgeneau, and G. Shirane, J. Phys. Soc. Jpn. **74**, 3002 (2005).

[45] C. Stock, R.J. Birgeneau, S. Wakimoto, J.S. Gardner, W.Chen, Z.-G. Ye, and G. Shirane, Phys. Rev. B **69**, 094104 (2004).

[46] B. Dkhil, J.M. Kiat, G. Calvarin, G. Baldinozzi, S.B. Vakhrushev, and E. Suard, Phys. Rev. B **65**, 024104 (2001).

[47] Throughout this paper we define the penetration depth as the distance at which the beam intensity is reduced by $1/e$ of its original value.

[48] G. Xu, D. Viehland, J.F. Li, P.M. Gehring, and G. Shirane Phys. Rev. B **68**, 212410 (2003).

[49] K. H. Conlon, H. Luo, D. Viehland, J.F. Li, T. Whan, J.H. Fox, C. Stock, and G. Shirane, Phys. Rev. B **70**, 172204 (2004).

[50] G. Xu, P. M. Gehring, C. Stock, and K. Conlon, Phase Transitions **79**, 135 (2006). G. Xu, Z. Zhong, Y. Bing, Z.-G. Ye, C. Stock, and G. Shirane, Phys. Rev. B **70**, 064107 (2004). G. Xu, Z. Zhong, Y. Bing, Z.-G. Ye, C. Stock, and G. Shirane Phys. Rev. B **67**, 104102 (2003).

[51] P.M. Gehring, W. Chen, Z.-G. Ye, and G. Shirane, J. Phys: Condens. Matter **16**, 7113 (2004).

[52] A. Lebon, H. Dammak, G. Calvarin, and I.O. Ahmedou J. Phys.: Condens. Matter **14**, 7035 (2002).

[53] V.Y. Shvartsman, Phys. Rev. B **71**, 134103 (2005).

[54] V.Y. Shvartsman and A.L. Kholkin, J. Appl. Phys. **101**, 064108 (2007).

[55] K. Hirota, G. Shirane, P.M. Gehring, and C.F. Majkrzak, Phys. Rev. B **49**, 11967 (1994).

[56] P.M. Gehring, K. Hirota, C.F. Majkrzak, Phys. Rev. Lett. **71**, 1087 (1993).

[57] R.A. Cowley and G. Shirane, J. Phys. C **11**, L939 (1978).

[58] Y.J. Wang, Y.-J. Kim, R.J. Christianson, S.C. LaMarra, F.C. Chou, and R.J. Birgeneau, Phys. Rev. B **63**, 052502 (2001).

[59] R.A. Cowley, Physica Scripta T66, 24 (1996).

PMN, E_i=14.7 meV, Q=(111)

a)

○ 0 kV/cm
■ 4 kV/cm
◇ 8 kV/cm

Strain × 10^{-3} (d/d$_0$)−1

b)

Γ/Γ_0

Temperature (Kelvin)

PMN, X–ray, Ei=10.7 keV